JPET Fast Forward. Published on June 14, 2006 as DOI: 10.1124/jpet.106.106757

THE KCNQ OPENER RETIGABINE INHIBITS THE ACTIVITY OF MESENCEPHALIC DOPAMINERGIC SYSTEMS OF THE RAT

Henrik H. Hansen, Christina Ebbesen, Claus Mathiesen, Pia Weikop, Lars Christian Rønn, Olivier Waroux, Jacqueline Scuvée-Moreau, Vincent Seutin[#], and Jens D. Mikkelsen[#*].

Department of Functional Neuroanatomy and Biomarkers (HHH, CE, JDM); Department of In Vivo Pharmacology (CM); Department of Microdialysis (PW), Department of Neurodegeneration and Repair (LCR), NeuroSearch A/S, Ballerup. Department of Pharmacology and Research Center for Cellular and Molecular Neurobiology, University of Liege, Belgium (OW, JSM, VS).

Running title*:* KCNQ channels modulate dopaminergic neurotransmission

Corresponding author: Jens D. Mikkelsen, MD PhD

NeuroSearch A/S

Pederstrupvej 93, DK-2750 Ballerup, Denmark

Phone: +45 44608359, Fax: +45 44608080

E-mail: JDM@Neurosearch.dk

Document statistics: No. of text pages: 41

No. of figures: 10

No. of references: 40

No. of words: Abstract:211

Introduction:436

Discussion:1,373

Abbreviations:

ABC, avidin-biotin complex reaction; ACCshell, shell subpart of the nucleus accumbens; ACCcore, core subpart of the nucleus accumbens; ACSF, artificial cerebrospinal fluid; BSA, bovine serum albumin; COMT, catechol-*O*-methyltransferase; DA, dopamine; DAB, diaminobenzidine tetrahydrochloride; DMSO, dimethyl sulphoxide; DOPAC, 3,4-dihydroxyphenylacetic acid; $GABA_A$ receptor, γ-amino-butyric-acid receptor subtype A; HVA, homovanillic acid; I_h

channel, hyperpolarization-activated channel; KCNQ, Kv7 channel; mAHP, medium afterhyperpolarisation phase; MAO, monoamine-oxidase; PBS, phosphate buffered saline; P-TH, phospho-tyrosine hydroxylase (Ser40); SK channel, small-conductance calcium-activated K+ channel; SN, substantia nigra; SNc, substantia nigra pars compacta; SNr, substantia nigra pars reticulata; SR95531, 2-(3'-carbethoxy-2'-propenyl)-3-amino-6-paramethoxy-phenyl-pyridazinium bromide; STRdl, dorsolateral part of the rostral striatum; TBS-T, Tris-buffered saline-Tween-20 solution, TH, tyrosine hydroxylase; TX, Triton X-100; VTA, ventral tegmental area; XE991, 4-pyridinylmethyl-9(10H)-anthracenone; ZD7288, 4-(N-ethyl-N-phenylamino)-1,2-dimethyl-6-(methylamino) pyridinium chloride.

JPET Fast Forward. Published on June 14, 2006 as DOI: 10.1124/jpet.106.106757
This article has not been copyedited and formatted. The final version may differ from this version.

Abstract

Homo- and heteromeric complexes of KCNQ subunits are the molecular correlate of the M-current, a neuron-specific voltage-dependent K^+ current with a well-established role in control of neural excitability. We investigated the effect of KCNQ channel modulators on the activity of dopaminergic neurons *in vitro* and *in vivo* in the rat ventral mesencephalon. The firing of dopaminergic neurons recorded in mesencephalic slices was robustly inhibited in a concentration-dependent manner by the KCNQ opener, retigabine. The effect of retigabine persisted in the presence of tetrodotoxin and simultanous blockade of $GABA_A$ receptors, SK and I_h channels, and was potently reversed by the KCNQ channel blocker XE991, indicating a direct effect on KCNQ channels. Similarly, *in vivo* single unit recordings from dopaminergic neurons revealed a prominent reduction in spike activity after systemic administration of retigabine. Furthermore, retigabine inhibited dopamine synthesis and c-Fos expression in the striatum under basal conditions. Retigabine completely blocked the excitatory effect of dopamine D_2 autoreceptor antagonists. Again, the in vitro and in vivo effects of retigabine were completely reversed by pre-administration of XE991. Dual-immunocytochemistry revealed that KCNQ4 is the major KCNQ subunit expressed in all dopaminergic neurons in the mesolimbic and nigrostriatal pathways. Collectively, these observations indicate that retigabine negatively modulates dopaminergic neurotransmission, likely originating from stimulation of mesencephalic KCNQ4 channels.

Introduction

KCNQ (also termed Kv7) channels are voltage-dependent potassium channels composed of homo- and heteromeric complexes of five different KCNQ subunits (KCNQ1-5, Kv7.1-Kv7.5). Unlike KCNQ1, all other KCNQ subunits (KCNQ2-5) are expressed in the CNS (Jentsch, 2000). Opening of KCNQ channels leads to neuronal hyperpolarization, thereby stabilizing the membrane potential and decreasing excitability. This makes them particularly interesting as targets in CNS diseases linked to hyperexcitability, including epilepsy, anxiety, pain and migraine (Blackburn-Munro, et al., 2005). The attractiveness of neuronal KCNQ channels in the treatment of such disease states is strongly supported by the identification of mutations within the human KCNQ genes. Thus, mutations in the KCNQ2 and KCNQ3 genes are associated with benign familial neonatal convulsions (Biervert, et al., 1998), and certain mutations in the KCNQ4 gene results in progressive hearing loss (Kubisch, et al., 1999).

Several attempts have been made to find pharmacological KCNQ modulators. Retigabine [N-(2-amino-4-(4-fluorobenzylamino)-phenyl) carbamic acid ethyl ester] was the first KCNQ opener to be reported and is now in development as an anti-epileptic compound (Blackburn-Munro, et al., 2005). *In vitro*, retigabine increases open-probability of KCNQ channels by shifting the voltage-dependence to more negative voltages (Tatulian, et al., 2001). This underlies the hyperpolarization and reduced firing frequency produced by the drug in various neuronal populations, including hippocampal and sympathetic neurons (Passmore, et al., 2003; Yue and Yaari, 2004). In these cell types, retigabine is thought to exert its inhibitory action by binding to KCNQ2/3 channels, as this KCNQ channel heteromer is expressed in

significant quantities compared to other KCNQ channel subunit combinations (Cooper, et al., 2001; Passmore, et al., 2003).

However, KCNQ channels also modulate the excitability of other cell types in the CNS. Thus, we have recently shown that retigabine profoundly inhibits haloperidol-induced c-Fos expression in the striatum (Mikkelsen, 2004), but have not determined the site of action within the basal ganglia. Additionally, flupirtine, a structural analogue of retigabine, is reported to inhibit haloperidol-induced catalepsy (Schmidt, et al., 1997). Haloperidol-induced striatal c-Fos activation and catalepsy are hallmarks of acute blockade of dopamine (DA) D_2 autoreceptors (Robertson and Fibiger, 1992), suggesting that retigabine interferes with DA neurotransmission.

We therefore aimed at localizing the target area and the mechanism of action for retigabine's pronounced inhibitory effect on striatal excitability.

Using a range of immunohistochemical techniques, *in vivo* and *in vitro* electrophysiological recordings as well as *in vivo* microdialysis, we demonstrate that KCNQ channel stimulation profoundly inhibits neuronal excitability in mesencephalic neurons which resulted in reduced DA activity in the striatum. This effect likely originates from stimulation of KCNQ4 channels located on DA neurons in the substantia nigra pars compacta and ventral tegmental area.

JPET Fast Forward. Published on June 14, 2006 as DOI: 10.1124/jpet.106.106757
This article has not been copyedited and formatted. The final version may differ from this version.

Methods

Animals

Unless stated specifically, adult male Wistar rats weighing 250-300 grams were used. All experiments were conducted in accordance with guidelines of the National Institute of Health (NIH Publications No. 85-23, 1985) and the Animal Experimentation Inspectorate, Ministry of Justice, Denmark.

Immunocytochemical staining of KCNQ subunits in the ventral tegmentum

For immunocytochemistry, the rats were anaesthetized with mebumal (50 mg/ml, 3 ml/kg) perfused with 0.1 M phosphate buffered saline (PBS; pH 7.4) followed by fixation in 4% paraformaldehyde-PBS for 10 minutes, excised and finally immersed in the fixative for 16 hours at 4°C. The brains were cryoprotected in 20% sucrose-PBS for 48 hours prior to sectioning. Forty micron serial frontal sections were cut in series of six through the mesencephalon. Prior to the immunocytochemical steps, the sections were rinsed for 3 x 10 min in 0.01M PBS, for 10 min in 1% H_2O_2–PBS to block endogenous peroxidase activity, and for 30 min in 0.01M PBS with 0.3% Triton X-100 (TX, Sigma, St. Louis, MI, USA), 5% swine serum, and 1% bovine serum albumin (BSA) to block non-specific binding sites. The sections were then incubated at 4°C for 24 hours in antisera against KCNQ2 (1:1,000) (Cooper, et al., 2001), KCNQ3 (1:1,000) (Sigma, St. Louis, MI, USA), KCNQ4 (1:5,000)(Kharkovets, et al., 2000), or KCNQ5 (1:1,000) (Yus-Najera, et al., 2003). The antisera were diluted in 0.01M PBS to which 0.3% Triton X-100 and 1% BSA was added.

After incubation in primary antiserum, immunoreactivity was detected by means of the avidin-biotin method using diaminobenzidine (DAB) as chromagen according to

previously described methods (Cooper, et al., 2001). Briefly, the sections were washed in PBS with 0.1% TX, and incubated for 60 minutes in biotinylated donkey anti-rabbit (Jackson Laboratories, Ben Harbor, ME) diluted 1:800 in PBS with 1% BSA, washed again and transferred to the avidin-biotin complex reaction (ABC, Vector Laboratories, Burlingame, CA) diluted 1:250 in PBS-TX. For KCNQ4, the tyramide amplification method was applied by subsequently incubating sections in biotinylated tyramide for 10 min (10 μl/ml PBS + 0.1% TX + 0.005% H_2O_2) and thereafter transferred to the ABC complex for additional staining.

Finally, after a careful wash the sections were incubated in 0.05% DAB (Sigma, St. Louis, MI, USA) with 0.05% H_2O_2 in PBS buffer for 10 minutes and then washed twice in PBS buffer. The sections were mounted on gelatinised glass slides, dried, and coverslipped in Depex.

Double labeling immunocytochemistry

For immunoflorescence colocalisation studies, a mixture of a monoclonal antibody against tyrosine hydroxylase (TH, 1:5000, DiaSorin, Stillwater, MN) and anti-KCNQ4 (1:1,000) was used. Subsequently, the sections were washed and incubated in a mixture of biotinylated donkey anti-rabbit (1:800) and Alexa Cy3-conjugated sheep anti-mouse (1:200, Invitrogen, Carlsbad, CA). The immunoreactions for KCNQ4 were completed using the tyramide-biotin procedure as described above with fluorescent avidin D (1:200, Vector Laboratories, Burlingame, CA). The sections were mounted on cleaned slides using a fluorescence mounting medium (DAKO Cytomation, Glostrup, Denmark) and visualised using confocal microscopy. Figures of representative photomicrographs were prepared using Adobe Photoshop CS (Adobe Systems, Mountain View, CA).

Extracellular electrophysiological recordings on rat midbrain slices

The method used has been described previously (Seutin, et al., 1990). Briefly, male Wistar rats (150-200 g) were anaesthetized with chloral hydrate (400 mg/kg, i.p., Sigma, St. Louis, MI, USA) and decapitated. The brain was rapidly removed and placed in cold (~ 4°C) artificial cerebro-spinal fluid (ACSF) of the following composition (in mM): NaCl 130, KCl 3.5, NaH_2PO_4 1.25, $MgSO_4$ 1.25, $CaCl_2$ 2, glucose 10, $NaHCO_3$ 24, saturated with 95% O_2 and 5% CO_2 (pH 7.4). A block of tissue containing the midbrain was placed in a vibratome filled with ice-cold ACSF and cut in 400 μm thick horizontal slices. The mesencephalic slice was placed on a nylon mesh in a recording chamber (volume of 500 μl). The tissue was held in position with an electron microscopy grid weighed down by short pieces of platinum wire. The slice was completely immersed in a continuously flowing (~ 2 ml/min), heated solution (34.5 ± 0.5° C) of ACSF. The substantia nigra (SN) was identified by transillumination as a semi-lucent area rostral to the medial terminal nucleus of the accessory optic tract (Paxinos and Watson, 1986). Additional experiments on the ventral tegmental area (VTA) were performed in the lateral part.

Extracellular single-cell recordings were made using glass microelectrodes filled with ACSF (resistance 5 to 10 MΩ). Action potentials were amplified and displayed on a Fluke digital oscilloscope (model PM 3370B). They were selected with a window discriminator and counted with a digital counter. They were also fed to an analog digital interface (CED1401) connected to a computer. Data were collected and analysed with the use of the Spike2 v.4 software (Cambridge Electronic Design, Cambridge, UK).

DA neurons in the substantia nigra pars compacta (SNc) recorded *in vitro* are characterized by long duration, often triphasic action potentials (≥ 2.5 ms) and a

regular firing rate of 0.5 to 4 spikes/s. They are inhibited by nanomolar concentrations of the DA D_2 receptor agonists BHT-920, apomorphine, or quinpirole. In all experiments, a 5 min control period was taken to assess the stability of the cells. Drugs were then superfused using three-way taps so that the flow rate remained constant. Each concentration was superfused until equilibrium was obtained (duration: usually 10 to 15 min). For each concentration, the percent inhibition relative to the mean control period firing rate was calculated and the concentration producing 50% inhibition (IC_{50}) was determined for each cell. When antagonists/channel blockers were tested they were first superfused alone for 10 minutes prior to testing their ability to block the effect of agonists/channel openers.

Intracellular recordings in rat midbrain slices

The method for the rat midbrain slice preparation is similar to that described for extracellular electrophysiological recordings, as described above. Intracellular recordings were made using glass microelectrodes filled with 2 M KCl (resistance 70 to 150 MΩ). All recordings were made in the bridge balance mode, using an NPI SEC1L amplifier (NPI Electronic GmbH, Tamm, Germany). The accuracy of the bridge was checked throughout the experiments by examining the voltage deflection induced by a small (±50 pA) current injection. The potential of the extracellular medium was measured at the end of each experiment and its absolute value was within 5 mV of that set to zero at the start. Membrane potentials and injected currents were recorded on a Gould TA240 chart recorder (Gould Instrument Systems, Valley View, OH) and on a Fluke Combiscope oscilloscope (Fluke Corp., Everett, WA). The Flukeview software was used for off-line analysis.

The characteristics of DA neurons recorded intracellularly have been described previously (Seutin, et al., 1997) and include a slow (0.5-4 Hz) regular pacemaker-like firing, a significant small-conductance calcium-activated K+ channel (SK) mediated afterhyperpolarization and a robust hyperpolarization-activated channel (I_h) mediated current.

All experiments were performed in the presence of 0.5 µM tetrodotoxin (TTX, Sigma, St. Louis, MI, USA) in order to minimize indirect effects. In addition, in a few experiments, the I_h blocker ZD7288 [4-(N-ethyl-N-phenylamino)-1,2-dimethyl-6-(methylamino) pyridinium chloride] (30 µM, Sigma, St. Louis, MI, USA) and the SK channel blocker apamin (300 nM, Sigma, St. Louis, MI, USA) were used. Finally, the $GABA_A$ antagonist SR95531 [2-(3'-carbethoxy-2'-propenyl)-3-amino-6-paramethoxy-phenyl-pyridazinium bromide] (10 µM, gift from Sanofi-Synthélabo, Paris, France) was also used in some experiments to exclude the possibility of an action of retigabine on these receptors (van Rijn and Willems-van, 2003).

The KCNQ channel blocker, XE991 [4-pyridinylmethyl-9(10H)-anthracenone], was synthesized at the Department of Medicinal Chemistry, NeuroSearch A/S, dissolved in DMSO (final concentration of DMSO: 0.1%) and applied by superfusion using three-way taps. Complete exchange of the bath solution occurred within 2-3 min.

In vivo single unit electrophysiology

Rats (n=8) were anaesthetized with chloral hydrate (400 mg/kg, i.p.) and mounted in a Kopf stereotaxic frame with the incisor bar set 3.75 mm below the interaural line. They were fitted with a catheter in the femoral vein to administer drugs (1.0 ml/kg) and supplementary anesthesia (80 mg/kg, i.v.). Body temperature was monitored by a rectal thermometer and maintained at 36.5-37.0°C with a thermostatically controlled

heating pad. An incision was made in the scalp, the skull was exposed, and a burr whole drilled overlying the SN. The dura mater was retracted and a glass microelectrode (filled with 2 M NaCl) was used to perform extracellular single unit recordings from DA neurons in the SNc. Electrode penetrations were made through the SNc in the dorso-ventral direction from 6.0-8.0 mm below the dura, 3.0-3.3 mm anterior to the interaural line, and 2.2-2.4 mm lateral to the midline, respectively, according to Paxinos & Watson (1986). As previously reported, the DA neurons (1) exhibited a characteristic triphasic waveform with a long action potential of 2.5-3.5 msec, (2) had a low spontaneous firing rates of 0.5-10 Hz, and an irregular firing pattern, and (3) were inhibited by apomorphine (0.04 mg/kg, i.v., Sigma, St. Louis, MI, USA) (Grace and Bunney, 1980).

Baseline activity of DA cells was recorded for at least 3 minutes prior to intravenous drug administration. Haloperidol (0.08 mg/kg, i.v., Janssen-Cilag, Beerse, Belgium) was administered following recovery of the spike frequency after apomorphine treatment. Upon haloperidol administration, DA cell firing was allowed to reach a stable plateau before administering retigabine (2.5 mg/kg, i.v.) or vehicle (10% Tween-80 in 0.9% NaCl, i.v.). Firing rates were collected on-line via an interface (1401Plus, Cambridge Electronic Design, U.K) using the Spike2 software (Cambridge Electronic Design, U.K.). The total number of spikes was calculated every 10 seconds. In all experiments, only one cell per animal was monitored unilaterally for its response to drug administration. Recordings were averaged over a total time interval of 3 minutes and compared to the baseline activity defined as the mean spike level before the first drug injection. The statistical significance of the effect of haloperidol and retigabine, respectively, was determined by comparing the activity of the cell measured as the averaged spike frequency within a time period of 3 minutes

before drug administration and within 2-10 minutes after drug injection. The effect of drug exposure was analyzed using a one-way ANOVA followed by Tukey's post-hoc test.

Immunohistochemical analysis of c-Fos expression

Rats were injected intraperitoneally (i.p.) with a single dose of retigabine (10 mg/kg, dissolved in 10% Tween-80 in 0.9% NaCl, n=7) or vehicle (n=8). In order to examine the inhibitory role of retigabine, combinations of two drug substances or vehicle (n=6 per group) were given to each rat. Within a 15 minutes interval, each animal was injected with retigabine (0.1-10 mg/kg, dissolved in 10% Tween-80 in 0.9% NaCl) or vehicle followed by i.p. administration of either saline vehicle, haloperidol (1.0 mg/kg, dissolved in 0.9% NaCl), or raclopride (0.5 mg/kg, dissolved in 0.9% NaCl, Sigma, St. Louis, MI, USA). XE991 (3.0 mg/kg, dissolved in 10% Tween-80 in 0.9% NaCl) or vehicle (n = 6) was administrated 5 minutes prior to retigabine.

The animals were returned to their home cages, and 60 minutes after the injection of retigabine or corresponding vehicle they were deeply anaesthetized with mebumal (50 mg/ml, 3.0 ml/kg, SAD, Copenhagen, Denmark) and perfused transcardially with PBS followed by 4% paraformaldehyde in 0.1 M phosphate buffer for 10 min. For c-Fos immunocytochemistry, the forebrains were immersed in fixative overnight and subsequently submerged in 30% sucrose in PBS at 4°C for three days. Forty micron serial coronal sections were cut through the forebrain on a freezing microtome and representative sections were processed immunocytochemically according to the avidin-biotin immunocytochemical protocol reported earlier (Mikkelsen, et al., 1998). The primary polyclonal antiserum (1:4,000), characterized previously (Mikkelsen, et

al., 1998), was generated in rabbit against the N-terminal peptide similar to amino acids 2-17 of the rat c-Fos protein.

The number of c-Fos positive cells were counted by means of light microscopy (20x magnification) using a counting grid (500 x 500 µm) placed over the shell (ACCshell) and core (ACCcore) of nucleus accumbens, as well as the dorsolateral part of the rostral striatum (STRdl). The number of c-Fos positive cells was averaged from two adjacent sections of each animal, and statistical analysis was performed on group means ± S.E.M. using an unpaired t-test or one-way ANOVA with Tukey's post-hoc test where appropriate.

Protein analysis and immunoblotting

In order to determine the influence on an effector of DA synthesis an assay detecting the Ser40 phosphorylation level of tyrosine hydroxylase was applied (Håkansson, et al., 2004). In an initial experiment, rats (n=6 per group) were injected with haloperidol (1.0 mg/kg) and sacrificed at various time points after the injection (15, 30 or 60 min). As the maximal level of Ser40 phosphorylation of TH was observed 30 min post-treatment, this time point was used to determine any inhibitory effect of retigabine. Retigabine (10 mg/kg, i.p.) was administered 15 minutes prior to haloperidol (1.0 mg/kg, i.p.). The rats were sacrificed 30 minutes after haloperidol treatment and the left and right dorsolateral striatae were rapidly excised, pooled, and snap-frozen in liquid nitrogen and kept at -80° C until further processing. For Western blotting analysis, total protein was extracted using the Total Protein Extraction Kit (Chemicon, Temecula, USA), according to the manufacturer's instructions. The supernatant was collected and the protein concentration was determined using a modified Lowry method (DC Protein Assay Kit; Bio-Rad). Protein extracts (20 µg

per sample) and a pre-stained weight marker (Invitrogen, Carlsbad, CA) were denaturated in sample loading buffer (Invitrogen, Carlsbad, CA) under reducing conditions, separated by 10% SDS-PAGE and electrotransferred in transfer buffer (80 mM Tris-HCl. 39 mM glycine, 20% methanol) to a nitrocellulose membrane (0.2 μm pore, Protran, Schleicher & Schuell, Dassel, Germany). The membrane was rinsed with Tris-buffered saline solution added Tween-20 (TBS-T; 10 mM Tris, 150 mM NaCl, 0.1% Tween-20, pH 7.6) and treated with blocking solution (5% nonfat dry milk in TBS-T) for 2 hrs at room temperature to prevent nonspecific antibody binding. Equal loading and transfer of proteins were initially confirmed by staining the membrane with Ponceau-S solution (Fluka, Buchs, Switzerland). The membrane was incubated overnight at 4° C with a rabbit phospho-specific Ser40-tyrosine hydroxylase antibody (P-TH, 1:3,000, Chemicon, Temecula, CA) or TH (1:4,000) (Chemicon, Temecula, CA), respectively. Following incubation with anti-rabbit horseradish peroxidase-labeled secondary antibody (1:30,000, Amersham Biosciences, Piscataway, NJ) at room temperature for 2 hrs, the immunoreactive protein was visualized by an enhanced chemiluminescence system (Pierce, Rockford, IL, USA), and serial exposures were made on autoradiographic films (Amersham Biosciences, Piscataway, NJ). For control of loading and transfer efficacy, the membranes were stripped for 5 min. at 37° C using a commercial stripping reagent (Restore Western Blot Stripping Buffer, Pierce, Rockford, IL, USA), and reprobed with a rabbit polyclonal actin antibody (1:30,000, Sigma, St. Louis, MI, USA). Densitometric analyses of blots were performed using ImagePro 5.1 (Media Cybernetics, Silver Spring, MD, USA), and data were expressed as P-TH or TH, respectively, relative to the corresponding actin level.

JPET Fast Forward. Published on June 14, 2006 as DOI: 10.1124/jpet.106.106757
This article has not been copyedited and formatted. The final version may differ from this version.

Microdialysis of striatal dopamine and dopamine metabolites in the striatum

Each rat was anaesthetized with isoflurane (1.5% isoflurane in a mixture of 20% O_2 and NO_2) and placed in a stereotaxic frame. The anaesthesia was maintained and the rectal temperature continuously measured during the experiment. The CMA/12 microdialysis probe (CMA Microdialysis, Solna, Sweden) of 4 mm in length was placed unilaterally into striatum. The probe was placed at the following coordinates (mm): anterior-posterior +1.0, lateral 3.0 and ventral -6.0 (from the dura) (Paxinos and Watson, 1986). The probe was perfused at a flow rate of 2 µl/min with Ringer solution (147 mM NaCl, 4 mM KCl, and 2.3 mM $CaCl_2$, pH 6.5) immediately after the implantation. The first three samples were discarded, and the subsequent three samples were collected to determine the baseline of extracellular DA and the DA metabolites 3,4-dihydroxyphenylacetic acid (DOPAC), and homovanillic acid (HVA). Thereafter, retigabine (10 mg/kg, i.p., n=6) or vehicle (10% Tween-80 in 0.9% NaCl, n=10) was administered and the following samples (20 minutes each) were collected for a total of 180 min. The brain dialysates collected from the probe were used for separate analysis of DA, DOPAC and HVA. Only rats with a verified correct placement of the probe in the striatum were included in the study.

Concentrations of DA, DOPAC and HVA were determined by reversed-phase HPLC with electrochemical detection as described previously (Weikop, et al., 2004). The mean AUC (area-under-the curve) levels of DA, DOPAC and HVA, respectively, were calculated from the three last microdialysate fractions collected prior to retigabine administration, normalized to 100% and thus considered being the basal level. All subsequent DA, DOPAC, and HVA sample values are expressed as mean levels ± S.E.M. relative to the basal levels. Statistical analysis was carried out using a two-way ANOVA (treatment x time) with Bonferroni's post-hoc test.

Results

Localization of KCNQ subunits in the ventral tegmentum

We examined the anatomical, cellular, and subcellular localization of KCNQ subunits in the ventral mesencephalon using well-characterized antisera. Immunoreactivity for the KCNQ subunits were observed to be differentially distributed in the SN as well as in other parts of the brain, as reported recently (Kharkovets, et al., 2000; Cooper, et al., 2001; Yus-Najera, et al., 2003). Only KCNQ2 and KCNQ4 immunoreactivity was detected in the SN (Fig. 1A-D). Bright-field microscopy revealed the presence of KCNQ2 immunoreactive neurons in both the SNc and SN pars reticulata (SNr) compartments, however, it was evident that more KCNQ-immunopositive neurons were present in the SNr than in the SNc (Fig. 1A). Relatively few KCNQ2-expressing neurons were found in the VTA (Fig. 1A). KCNQ4-positive neurons were widely distributed in the SNc and the adjacent VTA with an extensive number of KCNQ4-positive neurons in both regions (Fig. 1C). A few KCNQ4-positive neurons were present in the SNr (Fig. 1C).

KCNQ4 immunoreactivity seemed to overlap with DA cell rich areas, *i.e.* in the SNc, the VTA and the overlying A8 cell group in the retrorubral area, but not in other parts of the ventral mesenchephalon. Confocal immunofluorescence microscopy of sections co-stained for KCNQ4 and TH revealed that these two antigens completely overlapped in the SNc (Figs. 1E-G) and VTA (not shown). As indicated in Fig. 1F, the KCNQ4-labeled profile was observed not only in relation to plasma membranes, but was also found intracellular and in primary processes, whereas TH-immunoreactivity was more homogenously distributed in the cytoplasm.

JPET Fast Forward. Published on June 14, 2006 as DOI: 10.1124/jpet.106.106757
This article has not been copyedited and formatted. The final version may differ from this version.

Effect of retigabine and XE991 on midbrain dopamine cell firing *in vitro*:

Extracellular recordings

Retigabine exhibited a potent and robust inhibitory action on neuronal firing of DA neurons in the SNc (Fig. 2A). Thus, 1 μM retigabine significantly inhibited basal spike frequency and a concentration of 5 μM completely blocked neuronal firing (Fig. 2A). The IC_{50} of retigabine was 2.1±0.4 μM (n=10).

To determine the target specificity of retigabine, XE991 (1 μM) was added to the slice preparation under incrementing concentrations of retigabine. Application of retigabine in a concentration (10 μM) that completely blocks spike activity when applied alone had no activity when co-applied with XE991 (Fig. 2B). Only very high concentrations of retigabine could overcome the blockade by XE991 (Fig. 2B). The IC_{50} of retigabine in the presence of XE991 (1 μM) was 192±40 μM (n=6). Thus, 1 μM XE991 shifted the IC_{50} value of retigabine 91-fold. XE991 inhibited retigabine at even lower concentrations, since at 100 nM, it still shifted the IC_{50} value of retigabine significantly (6.2±1.2 μM in control conditions versus 2.1±0.4 μM, n=6, p=00072). Further quantitative analysis of the antagonism of retigabine by XE991, revealed that the 'K_B'-value (in analogy with receptor pharmacology: the concentration which doubles the IC_{50} of retigabine) of XE991 was 66 nM (Fig. 2C). Interestingly, XE991 produced a modest, but significant, increase (22%) of spike frequency (p=0.007, t-test, Fig. 2B).

In the VTA, retigabine also displayed an inhibitory effect on the basal spike activity. The IC_{50} of retigabine was 1.7 μM ± 0.4 μM (n=5, Fig 2D), and was not different from the IC_{50} of retigabine in SNc slice preparations (p=0.53). The inhibitory effect of retigabine in the VTA was completely blocked by XE991 (1 μM, n=2) (Fig 2D).

JPET Fast Forward. Published on June 14, 2006 as DOI: 10.1124/jpet.106.106757
This article has not been copyedited and formatted. The final version may differ from this version.

D_2 receptor antagonists (haloperidol, raclopride, 1 µM) had no significant influence on the basal DA neuron firing rate in rat midbrain slices, and did not change the effect of retigabine when co-applied (not shown).

Effect of retigabine and XE991 on midbrain dopamine cell firing *in vitro*:

Intracellular recordings

For intracellular recordings, the effect of retigabine was assessed in five SNc DA neurons. In two neurons, the experiments were performed in the presence of TTX. In three other neurons, the $GABA_A$ antagonist SR95531, the I_h blocker ZD7288 and the SK channel blocker apamin were also added to the control superfusion medium. Since no difference was observed between the two conditions, the results were pooled. The initial membrane potential was set at -50 mV by small DC current injections (+20 to -70 pA). 10 µM retigabine induced a hyperpolarization of 9.4±2.0 mV (Fig. 3A) (n=5). When the membrane potential was brought back to its initial value by current injection, a 54% drop in input resistance was observed (from 226 ± 46 to 102±13 MΩ). As shown in Fig. 3A, this effect was maintained during the superfusion of the drug and was only slowly reversible after wash-out. These effects of retigabine were completely blocked by the simultaneous application of 10 µM XE991 (n=3, Fig. 3B). XE991 had very little effect on the membrane potential when it was applied alone (not shown). At -80 mV, retigabine did not induce a hyperpolarization.

A final set of experiments was performed with XE991. At 10 µM, the KCNQ channel blocker did not modify the action potential amplitude (59.2±2 mV in control condition vs. 59.1±2 mV with XE991) or duration (0.97±0.1 ms in control condition vs. 1.0±0.1 ms with XE991). Also, XE991 (10 µM) did not induce significant changes in the membrane potential (Fig. 4A), and had no influence on the medium

afterhyperpolarization (mAHP) phase displayed by DA neurons (Fig. 4B), which is mediated by SK3 channels (Shepard and Bunney, 1991; Wolfart, et al., 2001). However, XE991 (10 μM) induced an increase in the number of spikes produced by depolarizing pulses (≥800 ms) in three out of six SNc DA neurons (Fig. 4C).

Effect of retigabine on SNc dopamine cell firing *in vivo*

Single unit recordings were employed to determine the effect of retigabine on SNc DA neuron firing *in vivo*. The neurons used for further characterization were selected if they displayed efficient firing inhibition by administration of the D_2 receptor agonist apomorphine, and excitation following treatment with haloperidol due to acute D_2 receptor blockade (Fig. 5A). Retigabine (2.5 mg/kg, n=8) almost instantly reduced the firing rate in SNc DA neurons from 160 ± 19 spikes/10 sec (after haloperidol treatment) to 28±13 spikes/10 sec (after retigabine treatment), thus significantly reducing the enhanced spike activity induced by haloperidol ($p<0.0001$). Notably, retigabine reduced the spike activity to a level below baseline (basal, 84 ± 6 spikes/10 sec vs. retigabine, 28±13 spikes/10 sec, $p=0.0022$), even in the presence of haloperidol (Fig. 5A and 5B). The prominent inhibitory effect of retigabine on DA cell firing was sustained throughout the experiment, thus lasting more than 10 minutes (Fig. 5A and 5B).

Retigabine inhibits c-Fos activation in the striatum

Functional analysis of retigabine on striatal activity was performed using the immediate-early transcription factor c-Fos as a marker of postsynaptic neuronal excitation. The basal level of c-Fos expression varied in different parts of the striatum, with the highest level in the ACCshell (199±35, Fig.6E) and lower in the ACCcore

JPET Fast Forward. Published on June 14, 2006 as DOI: 10.1124/jpet.106.106757
This article has not been copyedited and formatted. The final version may differ from this version.

(70±26, Fig. 6I) and STRdl (50±13, Fig. 6A). Administration of retigabine alone produced a significant reduction in basal striatal c-Fos levels. Compared to basal levels in vehicle-treated rats, retigabine (10 mg/kg) reduced c-Fos levels to almost undetectable levels in the STRdl (6±4, p=0.0094, Fig. 6F) and ACCcore (26±10, p=0.0211, Fig. 6J), whereas basal c-Fos expression in the ACCshell (83±19, p=0.0153, Fig. 6B) was partially blocked by retigabine.

As expected, haloperidol induced an intense c-Fos immunoreactivity in all parts of the striatum examined (Fig. 6 and 7), *i.e.* the dorsolateral region (15-fold increase), ACCshell (2-fold increase), and ACCcore (7-fold increase). Pretreatment with retigabine inhibited haloperidol-induced c-Fos dose-dependently, being evident in all aspects of the striatum examined (Figs. 6 and 7), as the inhibition was prominent in both the dorsal striatum (Fig. 6A-D), as well as in ACCshell (Fig. 6E-H) and ACCcore (Fig. 6I-L), respectively. The lowest dose of retigabine in all segments of the striatum showing a statistically significant effect was 1.0 mg/kg.

In the ventral striatum, the haloperidol-activated neurons were organized in the characteristic patches (Fig. 6G). Notably, retigabine eliminated the accumbal patchy organization of the c-Fos immunopositive neurons (Fig. 6H,L).

The inhibition of haloperidol-induced c-Fos levels in the striatum was counteracted by XE991 pre-administration. In all striatal areas examined, the inhibitory effect of retigabine was reversed completely to a level indistinguishable from animals treated with haloperidol alone (Fig. 8A-C). When administered alone, XE991 had no effect on c-Fos expression in any striatal subregion examined (Fig. 8).

The selective D_2 receptor antagonist, raclopride, produced a prominent induction of c-Fos in the striatum, topographically and quantitatively similar to that of haloperidol The prominent stimulatory effect of raclopride in the ventral striatum was completely

blocked by pre-administration of retigabine (ACCshell, vehicle 200±50 ; raclopride 410±27; retigabine+raclopride 187±39, $p<0.001$; ACCcore, vehicle 80±45; raclopride 347±72; retigabine+raclopride 70±19, $p<0.001$), whereas the inhibitory effect of retigabine was only partial in the STRdl (vehicle 6±3; raclopride 802±129; retigabine+raclopride 255±106; $p=0.0057$).

Retigabine blocks induction of TH phosphorylation in the striatum

Western blot analysis indicated that acute haloperidol treatment stimulated Ser40 phosphorylation of TH in tissue extracts of the STRdl. TH Ser40 phosphorylation was significantly increased 30 minutes after haloperidol administration ($p=0.0012$), whereas TH Ser40 phosphorylation slightly, but non-significantly, stimulated at 15 and 60 minutes after haloperidol administration (Fig.9A). The short-term effect of haloperidol on TH phosphorylation is in agreement with previous reports (Salvatore, et al., 2000; Håkansson, et al., 2004). Hence, due to the clear time-dependent response on haloperidol-induced Ser40 phoshorylation, the effect of retigabine was monitored 30 minutes after haloperidol administration.

As illustrated in Figure 9B, retigabine had no effect on Ser40 phosphorylation *per se*, but completely reversed the stimulatory effect of haloperidol. Subsequent Western blot analysis of total TH levels using a phosphorylation-independent TH antibody indicated that neither haloperidol, retigabine, nor the retigabine-haloperidol combination, had any effect on total TH levels compared to control levels ($p=0.598$, one-way ANOVA).

Retigabine reduces extracellular levels of dopamine metabolites *in vivo*

In vivo microdialysis was used to measure the effects of retigabine on the level of DA and the corresponding DA metabolites in the striatum (Fig. 10). Administration of retigabine alone did not influence extracellular DA levels in the striatum ($p=0.6638$, Fig 10A). By contrast, the levels of the two principal DA metabolites DOPAC (Fig. 10B) and HVA (Fig. 10C) were significantly reduced during retigabine treatment ($p<0.0001$ for both metabolites). The retigabine-induced inhibitory effect on DOPAC and HVA levels declined gradually. For DOPAC, the reduction was statistically significant at 60 min. post-injection, whereas HVA levels were significantly decreased at 100 min., and the response on both DA metabolites continued to decline throughout the experiment.

Discussion

We here demonstrate that retigabine profoundly affects neuronal excitability in SNc DA neurons.

In vitro, the effect of retigabine was both robust and highly sensitive to the KCNQ channel blocker XE991, indicating that retigabine acted via activation of KCNQ channels. A similar and equipotent effect of retigabine was also observed in the VTA. Our intracellular recordings performed in the presence of TTX and during blockade of $GABA_A$ receptors, SK and I_h channels, exclude the possibility that the inhibitory effect of retigabine on the excitability of DA neurons is mediated by an indirect effect in the SNc or by another action of retigabine. The lack of effect at -80 mV is consistent with an action on an M-type current (Delmas and Brown, 2005).

In vivo, the single unit recordings confirmed the *in vitro* observations by showing that retigabine not only fully blocked haloperidol-induced increase in firing rate, but also efficiently reduced the basal firing activity of SNc DA neurons.

A XE991-sensitive, typical M-type current, has recently been demonstrated in dissociated VTA DA neurons (Koyama and Appel, 2006). Taken together, those voltage-clamp experiments and our extracellular recordings (both *in vitro* and *in vivo*) and intracellular recordings, demonstrate the existence of a retigabine- and XE991-sensitive M-current in mesencephalic DA neurons. Our experiments further demonstrate that this current can be potentiated by retigabine in physiological conditions.

XE991 alone had very little effect on the membrane potential of SNc DA neurons, and did not affect the mAHP. However, XE991 increased the excitability of a fraction of SNc DA neurons, an effect similar to that reported for VTA DA neurons (Koyama

and Appel, 2006). These observations suggests that KCNQ channels sustaining this current may be differently expressed among DA neurons, either in terms of channel density, subunit composition or subcellular distribution.

Because KCNQ-immunopositive neurons were found in the SN and VTA, the powerful effect of retigabine is most likely triggered locally within the ventral tegmentum. The SN and VTA neurons displayed subunit-restricted KCNQ-labeling, as only immunoreactivity for KCNQ2 and KCNQ4 was found. Also, the IC_{50} for tetraethylammonium measured in dissociated VTA DA neurons is reported to lie between the IC_{50} of KCNQ2 and KCNQ4 channels, whereas the IC_{50} of XE991 is closest to that of expressed KCNQ2 channels (Koyama and Appel, 2006). This is interesting, because KCNQ2 and KCNQ4 do not co-assemble *in vitro* to generate functional heteromeric channels (Kubisch, et al., 1999). The lack of KCNQ3 immunoreactivity likely rules out that KCNQ2 and KCNQ4 immunoreactivity in the ventral tegmentum represents heteromeric KCNQ channels, and they may therefore operate as homomers. In accordance, homomeric KCNQ2 and KCNQ4 channels are capable of generating potassium currents *in vitro* (Biervert, et al., 1998; Kubisch, et al., 1999).

KCNQ2 immunoreactivity was present throughout the SN, as also reported in the mouse (Cooper, et al., 2001). In contrast, KCNQ4 subunits were observed in the rat SNc, but not in the SNr. The KCNQ4 subunit was predominantly localized to the plasma membrane, however KCNQ4 immunoreactivity was also observed in intracellular and primary processes, being in agreement with Kharkovets et al. (2000). Presumably, these KCNQ4 channel proteins are retained as a consequence of incomplete trafficking to the plasma membrane or, alternatively, may be destined for

trafficking to axonal, dendritic, or perisynaptic sites, as suggested for KCNQ2 channels (Cooper, et al., 2001).

This restricted subregional localization of KCNQ4 subunits is in agreement with a report on murine KCNQ4 distribution (Kharkovets, et al., 2000). In the SNc and VTA, KCNQ2 channels were much less expressed than KCNQ4 channels, likely indicating that the KCNQ4 channel is the predominant KCNQ channel responsible for the strong inhibitory effect of retigabine on DA neurotransmission. This is further supported by the immunohistochemical analysis of the principal neuronal phenotype expressing KCNQ4 subunits in the SNc and VTA, revealing that all KCNQ4 channels were present on TH-positive neurons and that KCNQ4 immunoreactivity was extensive, as virtually all mesencephalic DA neurons expressed KCNQ4 channels. We therefore conclude that the mesencephalic homomeric KCNQ4 channel is the molecular target of retigabine leading to inhibition of DA neuron firing.

The strong inhibitory effect of retigabine on mesencephalic DA activity is intriguing. Since the SNc and the lateral VTA provide essential and extensive DA modulatory inputs to striatal and mesolimbic targets (Swanson, 1982), this suggests that KCNQ channel modulation occurs in both nigrostriatal and limbic pathways.

Accordingly, retigabine almost completely eliminated basal excitability in both the dorsolateral and ventral aspects of the striatum, as inferred by the reduced levels of basal c-Fos immunoreactivity, a transcriptional marker commonly used to map changes in synaptic neuronal activity (Morgan and Curran, 1991).

Additionally, retigabine reduced basal striatal DOPAC and HVA without affecting DA levels. Since metabolism of DA, by concerted action of monoamine-oxidase (MAO) and catechol-*O*-methyltransferase (COMT), results in DOPAC and HVA

production, changes in DA metabolite levels reflect altered DA synthesis rate and DA neuronal activity (Nissbrandt, et al., 1989; Di Giulio, et al., 1978), we can therefore conclude that retigabine reduced DA synthesis in striatal nerve terminals. In accordance, retigabine also reversed haloperidol-induced TH Ser40 phosphorylation, a presynaptic marker of stimulated striatal DA synthesis (Håkansson, et al., 2004), indicating that retigabine was also capable of normalizing striatal TH activity in conditions of stimulated DA activity.

Acute blockade of DA D_2 receptors effectively depolarizes SNc neurons *in vivo* (Bunney, et al., 1973) and leads to prominent striatal excitation by stimulating DA release (Di Chiara and Imperato, 1988), turnover (Zetterstrom, et al., 1986), and synthesis (Magnusson, et al., 1987).

Haloperidol caused a pronounced c-Fos induction in the ventral and lateral striatum, interpreted as enhanced neuronal activity caused by acute blockade of somatodendritic and terminal DA D_2 receptor function (Robertson and Fibiger, 1992). Retigabine completely eliminated the strong excitatory response to haloperidol with an ED_{50} of approximately 1 mg/kg, and also inhibited the effect of raclopride, emphazising the inhibitory effect of retigabine on D_2 receptor blockade-mediated excitation. The potency of retigabine is higher than found in behavioral studies, where minimum effective doses typically range from 3 to 10 mg/kg (Korsgaard, et al., 2005). The negative modulatory effect on haloperidol-induced c-Fos was KCNQ-specific, as XE991 completely reversed this effect. Because virtually all DA neurons in the SNc and VTA express D_2 receptors (Khan, et al., 1998), this may be of functional relevance to KCNQ channel physiology. The interaction with the D_2 receptor-mediated c-Fos response in the striatum is further emphasized by the

observation that flupirtine inhibits haloperidol-induced catalepsy, which is a typical extrapyramidal effect of generalized D_2 receptor blockade (Schmidt, et al., 1997). Furthermore, motor impairment is also observed in rats exposed to acute retigabine administration (Rostock, et al., 1996; Korsgaard, et al., 2005), which may thus directly relate to the potent inhibitory effect of retigabine on striatal excitability.

Although the functional consequences of systemic administration of retigabine likely occurs in the SNc and VTA, the striatal effect could potentially also be explained by actions independent on DA input from the SNc and VTA.

Striatal neurons express KCNQ2, KCNQ3 and KCNQ5, but not KCNQ4, channels (Cooper, et al., 2001; Shen, et al., 2005). Also, heteromeric KCNQ2/3 channels are suggested to provide inhibitory tonus on striatopallidal/striatonigral neurons (Shen, et al., 2005). Striatopallidal neurons express D_2 receptors (Gerfen, et al., 1990) and respond to excitatory D_2 receptor blockade (Robertson and Jian, 1995). Thus, retigabine may also affect neuronal excitability by direct action on striatopallidal neurons. However, as striatal c-Fos induction by pharmacological D_2 receptor blockade is critically dependent on mesolimbic DA inputs (Robertson, et al., 1992), this likely rules out that intrastriatal KCNQ channels contributed significantly to the inhibitory effect of retigabine.

Also, the cortex and corticostriatal projections express KCNQ channel subunits (Cooper, et al., 2001; Yus-Najera, et al., 2003), which tentatively suggests that KCNQ channels on corticostriatal projections may play a role in the control of striatal excitability.

In conclusion, the prominent inhibitory effect of KCNQ activation in nigrostriatal and mesolimbic pathways suggests that pharmacological enhancement of KCNQ function

may be a novel approach to improve conditions of DA overactivity in the basal ganglia. Consistent with the localization of KCNQ4 subunits on key sites for control of cerebral DA activity, homomeric KCNQ4 channels may represent a novel target for treating disease states characterized by abnormal DA neurotransmission, *e.g.* schizophrenia, attention deficit hyperactivity disorder, and drug abuse.

Acknowledgements

The authors would like to thank Tine Engelbrecht, Pia Rovsing Sandholm, Rigmor Jensen, Christina Rasmussen, Charlotte Petersen, and Laurent Massotte for skillful technical assistance. The KCNQ channel antibodies were kindly supplied by Dr. Ed Cooper (Dept. of Neurology, University of Pennsylvania Medical Center, Philadelphia, PA), Dr. Thomas Jentsch (ZMNH, Hamburg University, Hamburg, Germany), and Dr. Alvaro Villaroel (Unidad de Biofísica, CSIC, UPV/EHU, Bilbao, Spain).

References

Biervert C, Schroeder BC, Kubisch C, Berkovic SF, Propping P, Jentsch TJ and Steinlein OK (1998) A potassium channel mutation in neonatal human epilepsy. *Science* 279:403-406.

Blackburn-Munro G, by-Brown W, Mirza NR, Mikkelsen JD and Blackburn-Munro RE (2005) Retigabine: chemical synthesis to clinical application. *CNS Drug Rev* 11:1-20.

Bunney BS, Walters JR, Roth RH and Aghajanian GK (1973) Dopaminergic neurons: effect of antipsychotic drugs and amphetamine on single cell activity. *J Pharmacol Exp Ther* 185:560-571.

Cooper EC, Harrington E, Jan YN and Jan LY (2001) M channel KCNQ2 subunits are localized to key sites for control of neuronal network oscillations and synchronization in mouse brain. *J Neurosci* 21:9529-9540.

Di Chiara G and Imperato A (1988) Drugs abused by humans preferentially increase synaptic dopamine concentrations in the mesolimbic system of freely moving rats. *Proc Natl Acad Sci U S A* 85:5274-5278.

Di Giulio AM, Groppetti A, Cattabeni F, Galli CL, Maggi A, Algeri S and Ponzio F (1978) Significance of dopamine metabolites in the evaluation of drugs acting on dopaminergic neurons. *Eur J Pharmacol* 52:201-207.

Gerfen CR, Engber TM, Mahan LC, Susel Z, Chase TN, Monsma FJ, Jr. and Sibley DR (1990) D1 and D2 dopamine receptor-regulated gene expression of striatonigral and striatopallidal neurons. *Science* 250:1429-1432.

Grace AA and Bunney BS (1980) Nigral dopamine neurons: intracellular recording and identification with L-dopa injection and histofluorescence. *Science* 210:654-656.

Håkansson K, Pozzi L, Usiello A, Haycock J, Borrelli E and Fisone G (2004) Regulation of striatal tyrosine hydroxylase phosphorylation by acute and chronic haloperidol. *Eur J Neurosci* 20:1108-1112.

Jentsch TJ (2000) Neuronal KCNQ potassium channels: physiology and role in disease. *Nat Rev Neurosci* 1:21-30.

Khan ZU, Mrzljak L, Gutierrez A, de la CA and Goldman-Rakic PS (1998) Prominence of the dopamine D2 short isoform in dopaminergic pathways. *Proc Natl Acad Sci U S A* 95:7731-7736.

Kharkovets T, Hardelin JP, Safieddine S, Schweizer M, El-Amraoui A, Petit C and Jentsch TJ (2000) KCNQ4, a K+ channel mutated in a form of dominant deafness, is expressed in the inner ear and the central auditory pathway. *Proc Natl Acad Sci U S A* 97:4333-4338.

Korsgaard MP, Hartz BP, Brown WD, Ahring PK, Strobaek D and Mirza NR (2005) Anxiolytic Effects of Maxipost (BMS-204352) and Retigabine via Activation of Neuronal Kv7 Channels. *J Pharmacol Exp Ther* 314:282-292.

Koyama S and Appel SB (2006) Characterization of M-current in Ventral Tegmental Area Dopamine Neurons. *J Neurophysiol*.

Kubisch C, Schroeder BC, Friedrich T, Lutjohann B, El Amraoui A, Marlin S, Petit C and Jentsch TJ (1999) KCNQ4, a novel potassium channel expressed in sensory outer hair cells, is mutated in dominant deafness. *Cell* 96:437-446.

Magnusson O, Mohringe B and Fowler CJ (1987) Comparison of the effects of dopamine D1 and D2 receptor antagonists on rat striatal, limbic and nigral dopamine synthesis and utilisation. *J Neural Transm* 69:163-177.

Mikkelsen JD (2004) The KCNQ channel activator retigabine blocks haloperidol-induced c-Fos expression in the striatum of the rat. *Neurosci Lett* 362:240-243.

Mikkelsen JD, Vrang N and Mrosovsky N (1998) Expression of Fos in the circadian system following nonphotic stimulation. *Brain Res Bull* 47:367-376.

Morgan JI and Curran T (1991) Stimulus-transcription coupling in the nervous system: involvement of the inducible proto-oncogenes fos and jun. *Annu Rev Neurosci* 14:421-451.

Nissbrandt H, Sundstrom E, Jonsson G, Hjorth S and Carlsson A (1989) Synthesis and release of dopamine in rat brain: comparison between substantia nigra pars compacts, pars reticulata, and striatum. *J Neurochem* 52:1170-1182.

Passmore GM, Selyanko AA, Mistry M, Al Qatari M, Marsh SJ, Matthews EA, Dickenson AH, Brown TA, Burbidge SA, Main M and Brown DA (2003) KCNQ/M currents in sensory neurons: significance for pain therapy. *J Neurosci* 23:7227-7236.

Paxinos G and Watson W (1986) *The rat brain in stereotaxic coordinates*. Academic Press Ltd., London, UK, London.

Robertson GS and Fibiger HC (1992) Neuroleptics increase c-fos expression in the forebrain: contrasting effects of haloperidol and clozapine. *Neuroscience* 46:315-328.

Robertson GS and Jian M (1995) D1 and D2 dopamine receptors differentially increase Fos-like immunoreactivity in accumbal projections to the ventral pallidum and midbrain. *Neuroscience* 64:1019-1034.

Robertson GS, Vincent SR and Fibiger HC (1992) D1 and D2 dopamine receptors differentially regulate c-fos expression in striatonigral and striatopallidal neurons. *Neuroscience* 49:285-296.

Rostock A, Tober C, Rundfeldt C, Bartsch R, Engel J, Polymeropoulos EE, Kutscher B, Loscher W, Honack D, White HS and Wolf HH (1996) D-23129: a new anticonvulsant with a broad spectrum activity in animal models of epileptic seizures. *Epilepsy Res* 23:211-223.

Salvatore MF, Garcia-Espana A, Goldstein M, Deutch AY and Haycock JW (2000) Stoichiometry of tyrosine hydroxylase phosphorylation in the nigrostriatal and mesolimbic systems in vivo: effects of acute haloperidol and related compounds. *J Neurochem* 75:225-232.

Schmidt WJ, Schuster G, Wacker E and Pergande G (1997) Antiparkinsonian and other motor effects of flupirtine alone and in combination with dopaminergic drugs. *Eur J Pharmacol* 327:1-9.

Seutin V, Scuvee-Moreau J and Dresse A (1997) Evidence for a non-GABAergic action of quaternary salts of bicuculline on dopaminergic neurones. *Neuropharmacology* 36:1653-1657.

Seutin V, Scuvee-Moreau J, Giesbers I, Massotte L and Dresse A (1990) Effect of BHT 920 on monoaminergic neurons of the rat brain: an electrophysiological in vivo and in vitro study. *Naunyn Schmiedebergs Arch Pharmacol* 342:502-507.

Shen W, Hamilton SE, Nathanson NM and Surmeier DJ (2005) Cholinergic suppression of KCNQ channel currents enhances excitability of striatal medium spiny neurons. *J Neurosci* 25:7449-7458.

Shepard PD and Bunney BS (1991) Repetitive firing properties of putative dopamine-containing neurons in vitro: regulation by an apamin-sensitive Ca(2+)-activated K+ conductance. *Exp Brain Res* 86:141-150.

Swanson LW (1982) The projections of the ventral tegmental area and adjacent regions: a combined fluorescent retrograde tracer and immunofluorescence study in the rat. *Brain Res Bull* 9:321-353.

Tatulian L, Delmas P, Abogadie FC and Brown DA (2001) Activation of expressed KCNQ potassium currents and native neuronal M-type potassium currents by the anti-convulsant drug retigabine. *J Neurosci* 21:5535-5545.

van Rijn CM and Willems-van BE (2003) Synergy between retigabine and GABA in modulating the convulsant site of the GABAA receptor complex. *Eur J Pharmacol* 464:95-100.

Weikop P, Kehr J and Scheel-Kruger J (2004) The role of alpha1- and alpha2-adrenoreceptors on venlafaxine-induced elevation of extracellular serotonin, noradrenaline and dopamine levels in the rat prefrontal cortex and hippocampus. *J Psychopharmacol* 18:395-403.

Wolfart J, Neuhoff H, Franz O and Roeper J (2001) Differential expression of the small-conductance, calcium-activated potassium channel SK3 is critical for pacemaker control in dopaminergic midbrain neurons. *J Neurosci* 21:3443-3456.

Yue C and Yaari Y (2004) KCNQ/M channels control spike afterdepolarization and burst generation in hippocampal neurons. *J Neurosci* 24:4614-4624.

Yus-Najera E, Munoz A, Salvador N, Jensen BS, Rasmussen HB, Defelipe J and Villarroel A (2003) Localization of KCNQ5 in the normal and epileptic human temporal neocortex and hippocampal formation. *Neuroscience* 120:353-364.

Zetterstrom T, Sharp T and Ungerstedt U (1986) Effect of dopamine D-1 and D-2 receptor selective drugs on dopamine release and metabolism in rat striatum in vivo. *Naunyn Schmiedebergs Arch Pharmacol* 334:117-124.

Footnotes

# Vincent Seutin (VS) and Jens D. Mikkelsen (JDM) contributed equally to the work.

* This work was supported by the EU 6th framework programme (LSHM-CT-2004-503038) (HEH, CE, CM, PW, LCR) and by a grant from the FNRS (no. 9.4560.03) (OW, JSM, VS).

Legends for Figures

Fig. 1 Immunohistochemical localisation of KCNQ subunits in the rat mesencephalon. Coronal sections of the ventral tegmentum immunopositive for KCNQ2 (A), KCNQ3 (B), KCNQ4 (C) and KCNQ5 (D), respectively. Moderate level of KCNQ2-immunoreactivity is found in both the pars reticulata (SNr) and pars compacta (SNc) of substantia nigra. Confocal microscopy illustrates simultaneous detection of KCNQ4 (E) and tyrosine hydroxylase (F) immunoreactivity in the rat SNc. There is a complete overlap between TH- and KCNQ4-immunoreactivity in SNc DA neurons. The cellular distribution of KCNQ4 immunoreactivity demonstrates an accumulation in the cellular membrane (arrow). Scale bar = 500 μm (A-D); 10 μm (E-G).

Fig. 2 Retigabine inhibits firing of DA neurons in rat brain slice preparations of the SNc. (A) Significant reduction of neuronal activity is observed at retigabine concentrations of 2 μM, and spike activity was completely blocked at concentrations of 5 μM retigabine. ***$p<0.001$ (compared to DMSO). (B) The capacity of retigabine to inhibit spike activity of SNc was effectively diminished in the presence of the KCNQ blocker, XE991 (1 μM). Thus, only concentrations of at least 300 μM significantly reversed the effect of XE991. Note that XE991 alone induced a significant increase (22%) of spike frequency. ##$p<0.01$; ###$p<0.001$ (compared to control); ***$p<0.001$ (compared to XE991+DMSO). (C) XE991 at very low concentrations significantly antagonizes the effect of retigabine. By analogy with receptor pharmacology, plotting the log (r-1) ratio (r being the ratio of the IC_{50}'s of

retigabine in the presence and in the absence of XE991), reveals a straight line with an estimated 'K_B'-value (the concentration of XE991 which doubles the EC_{50} of retigabine) of 66 nM. (D) Retigabine displays a similar inhibitory effect in VTA slice preparations (upper trace) and XE991 completely blocks this effect (lower trace). Traces are from the same VTA DA cell (lower trace was recorded 15 min. after upper trace). Control experiments (not shown) have demonstrated that repeated applications of a given concentration of retigabine yield reproductive inhibition of VTA firing in control conditions.

Fig.3 The effect of retigabine is due to an enhancement of a M-type current in DA neurons. (A) Retigabine induces a steady hyperpolarization and a decrease in input resistance in a DA neuron. Membrane potential and injected currents are shown. (B) The effect of retigabine is completely antagonized by XE991. XE991 had very little effect *per se* on the membrane potential (not shown).

Fig.4 (A) The KCNQ channel blocker, XE991 (10 µM), does not modify the amplitude or duration (measured at mid-height) of action potentials recorded intracellularly in rat SNc DA neurons. (B) XE991 (10 µM) has no influence on the medium afterhyperpolarization (mAHP) phase displayed by SNc DA neurons. (C) XE991 (10 µM) induces an increase in the number of spikes produced by depolarizing pulses in a fraction of SNc DA neurons. Action potentials elicited in two different DA neurons by 1.4 s depolarizing current injections of increasing amplitude before (traces 1 and 3) and during application of 10 µM XE991 (traces 2 and 4). Membrane potential was set at -63 mV before drug application. XE991 did not have a significant effect on the

baseline membrane potential. Note that XE991 increased the excitability of one cell in trace (traces 1 and 2), while it did not modify the excitability of another cell (traces 3 and 4).

Fig. 5 Retigabine blocks DA neuron activity *in vivo*. A representative trace of a single unit recording from a SNc DA neuron, showing the characteristic short-lasting inhibitory profile of apomorphine (apo, 0.04 mg/kg, i.v.) on DA cell firing. Haloperidol (Hal, 0.08 mg/kg, i.v.) significantly increases cell firing which is completely blocked by retigabine (ret, 2.5 mg/kg, i.v.). $^{\#}p<0.05$; $^{\#\#}p<0.01$ (compared to vehicle), ***$p<0.001$ (compared to haloperidol).

Fig. 6 Retigabine strongly inhibits haloperidol-induced c-Fos in all parts of the striatum. Photomicrographs illustrating distribution of c-Fos expression in the dorsolateral striatum (A-D), the shell (E-H) and core (I-L) of nucleus accumbens, respectively. The photomicrographs represent vehicle (A, E, I), retigabine (B, F, J), haloperidol (C, G, K) and retigabine-haloperidol treatment (D, H, L), respectively. Scale bar = 200 μm.

Fig. 7 Quantitative assessment of the dose-related effect of retigabine (0.1 – 10 mg/kg) on haloperidol-induced (1.0 mg/kg, i.p.) c-Fos induction in the dorsolateral striatum (A), nucleus accumbens shell (B) and core (C). A letter not in common signifies a statistical difference ($p<0.05$) between treatments.

Fig. 8 The KCNQ antagonist XE991 (XE, 3.0 mg/kg) completely blocks retigabine's (Ret) inhibitory effect on haloperidol-induced (Hal) c-Fos expression in all

three parts of the striatum, *i.e* (A) dorsolateral striatum; nucleus accumbens, shell (B) and core (C). The rats were pre-treated with XE991 5 min before retigabine (1.0 mg/kg). A letter not in common signifies a statistical difference ($p<0.05$) between treatments.

Fig. 9 Haloperidol (Hal, 1.0 mg/kg, i.p.) stimulates Ser40 phosphorylation of tyrosine hydroxylase (TH) in the dorsolateral striatum of rats. The effect was time-dependent with a significant increase at 30 minutes (**$p<0.01$) (A). Retigabine (Ret, 10 mg/kg, i.p.) completely blocked the haloperidol-induced (1.0 mg/kg, i.p.) phosphorylation of TH (***$p<0.01$ vs. haloperidol). The inhibitory effect of retigabine on haloperidol-induced TH Ser40 phosphorylation was phosphorylation-specific, because retigabine did not influence total TH protein levels in the STRdl (not shown).

Fig. 10 Extracellular levels of DA (A), DOPAC (B), and HVA (C) in the rat striatum following systemic administration of retigabine (10 mg/kg, i.p., open circles) or vehicle (10% Tween-80 in saline, filled circles). Retigabine was administered 40 minutes (t=0) after microdialysis was initiated. Retigabine had no effect on extracellular DA levels in the striatum, but induced a significant drop in DOPAC ($p<0.0001$) and HVA ($p<0.0001$) levels which progressed throughout the experiment. *$p<0.05$; **$p<0.01$; ***$p<0.001$, two-way ANOVA with Bonferroni's post-hoc test. Histograms of cumulated (0-180 min.) DA, DOPAC and HVA levels (AUC ±S.E.M.), respectively, are inserted. ***$p<0.001$, unpaired t-test. All data are normalized to the mean

concentration sampled in a total of 60 minutes prior to vehicle or retigabine injection.

JPET Fast Forward. Published on June 14, 2006 as DOI: 10.1124/jpet.106.106757
This article has not been copyedited and formatted. The final version may differ from this version.

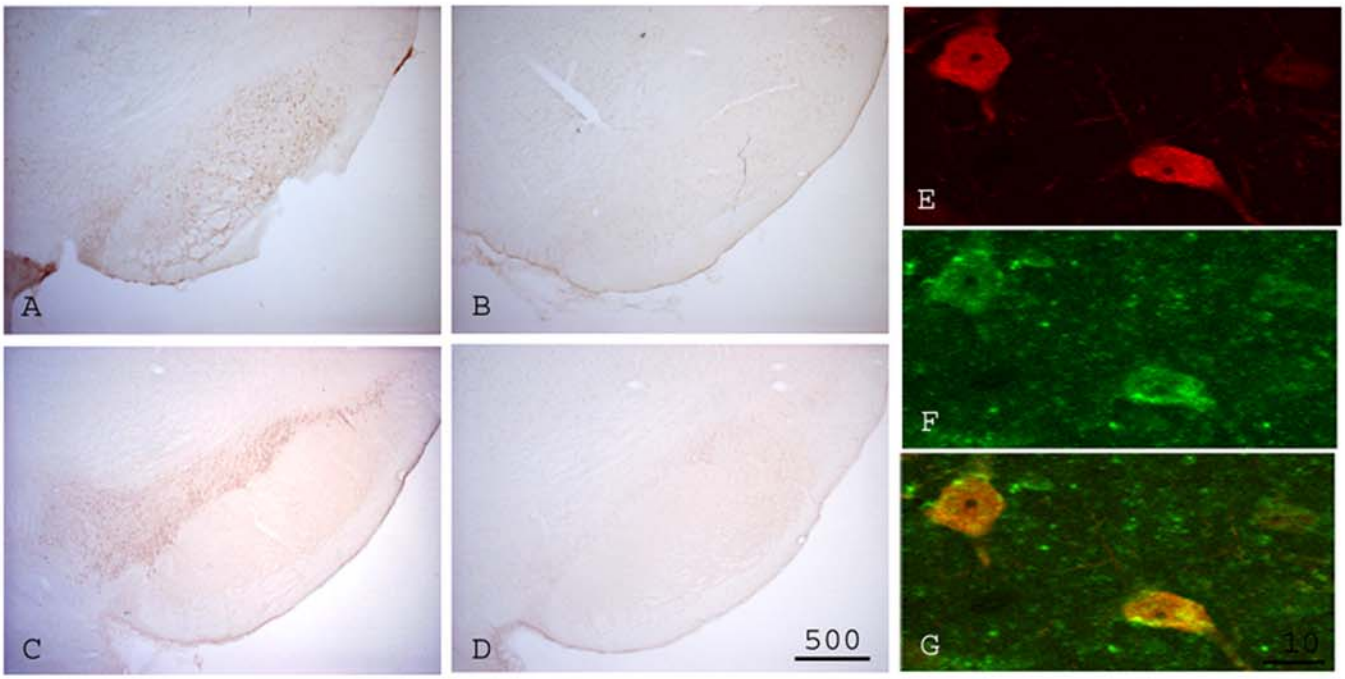

Figure 1

JPET Fast Forward. Published on June 14, 2006 as DOI: 10.1124/jpet.106.106757
This article has not been copyedited and formatted. The final version may differ from this version.

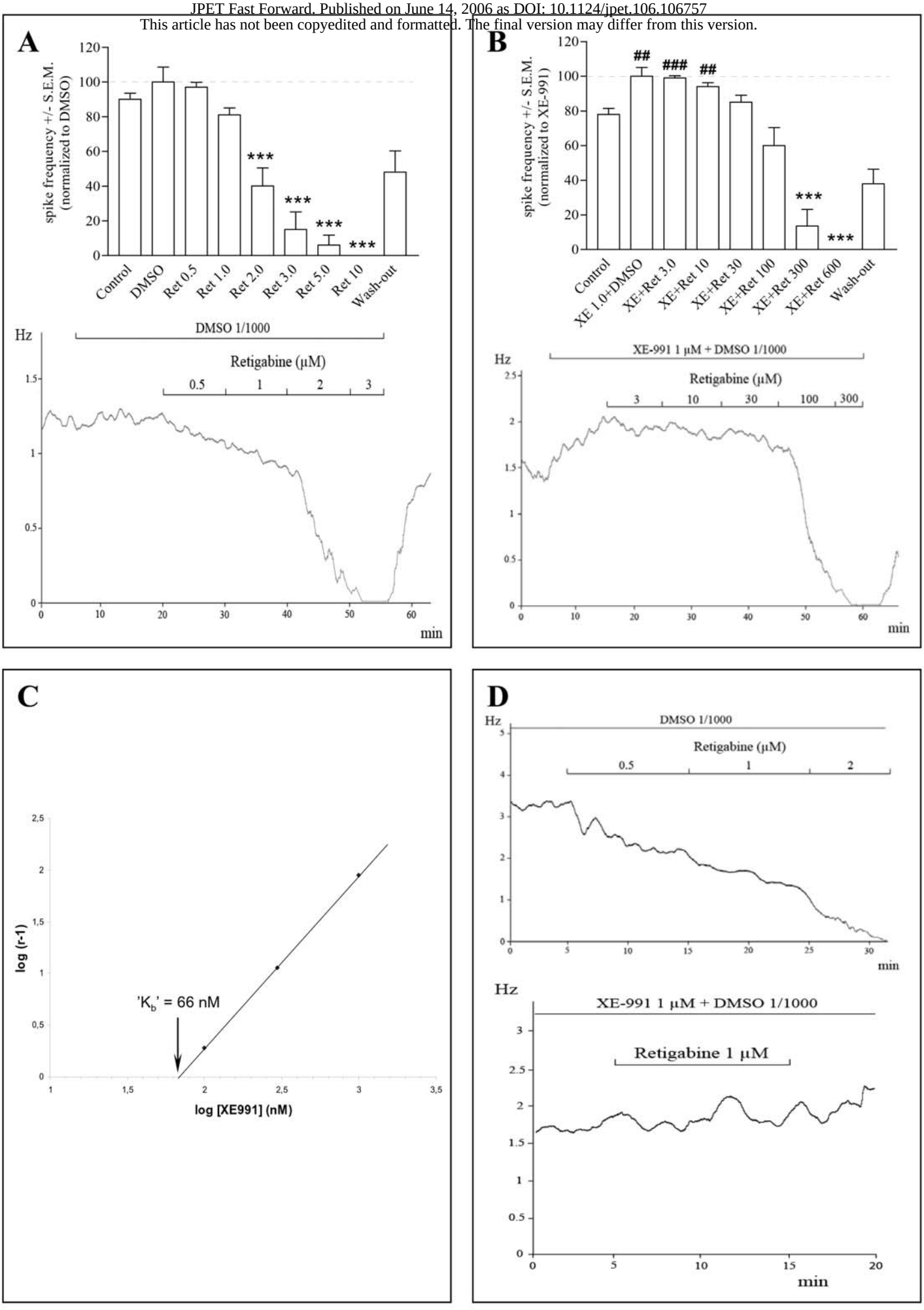

Figure 2

JPET Fast Forward. Published on June 14, 2006 as DOI: 10.1124/jpet.106.106757
This article has not been copyedited and formatted. The final version may differ from this version.

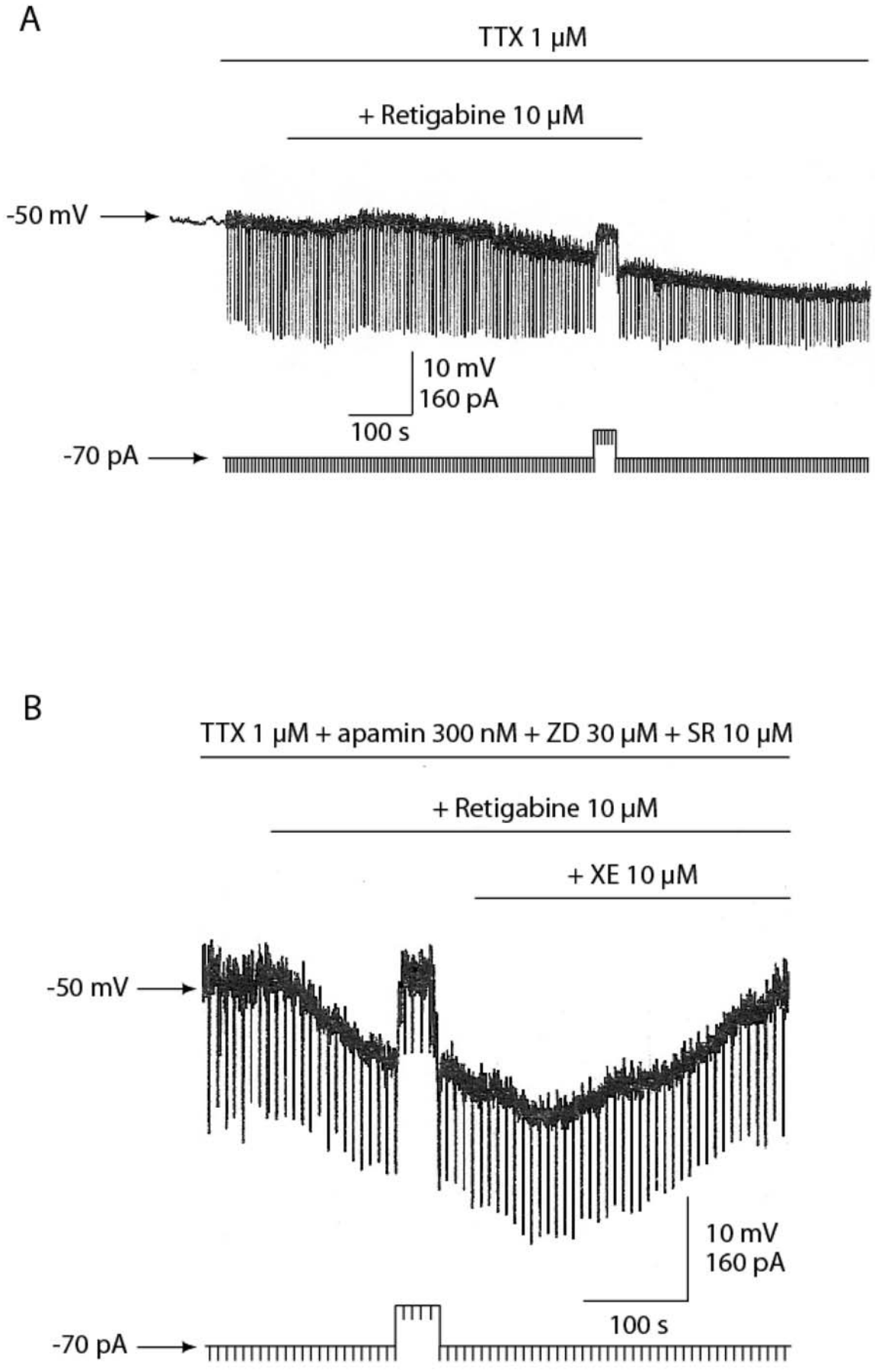

Figure 3

JPET Fast Forward. Published on June 14, 2006 as DOI: 10.1124/jpet.106.106757
This article has not been copyedited and formatted. The final version may differ from this version.

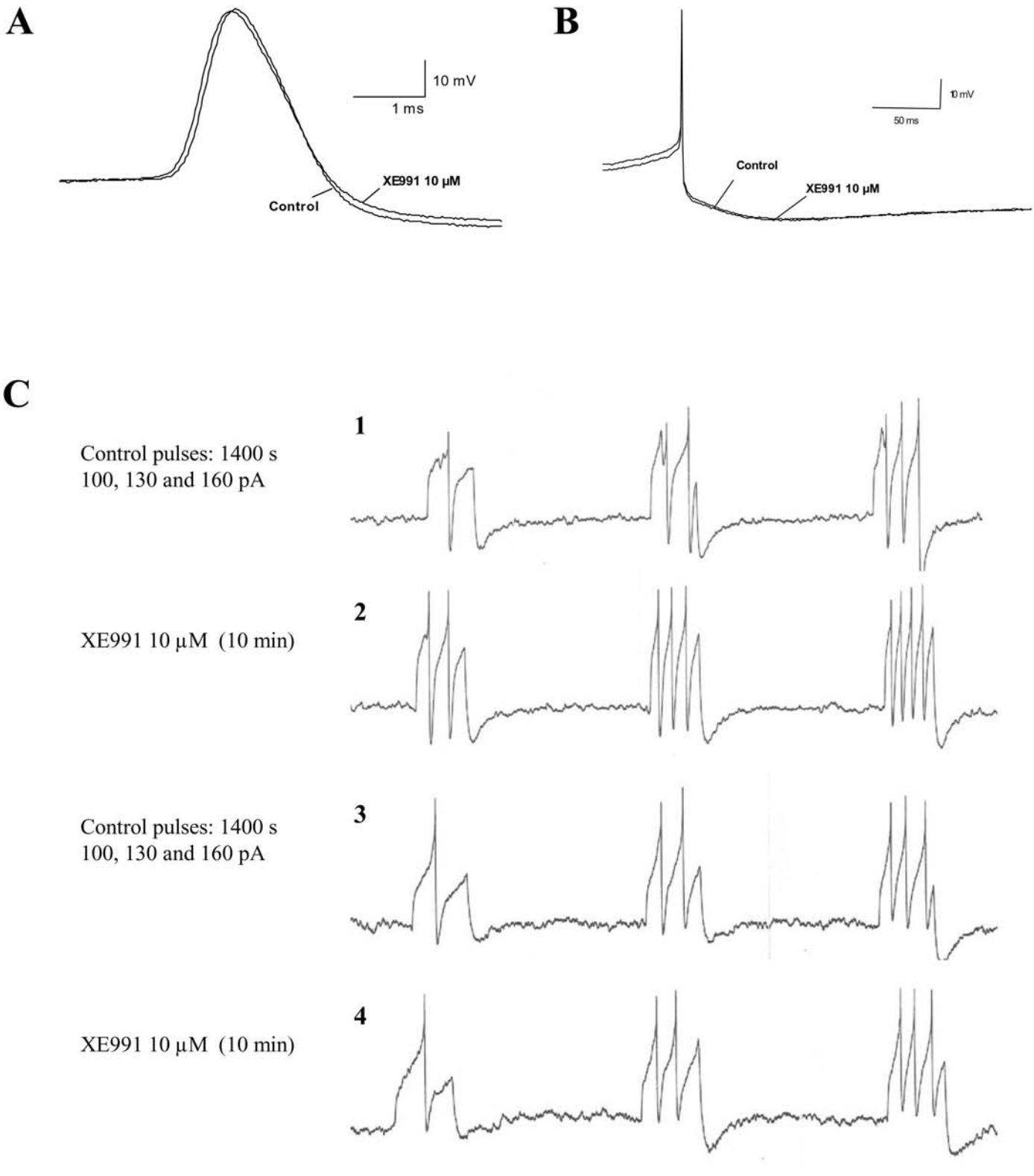

Figure 4

JPET Fast Forward. Published on June 14, 2006 as DOI: 10.1124/jpet.106.106757
This article has not been copyedited and formatted. The final version may differ from this version.

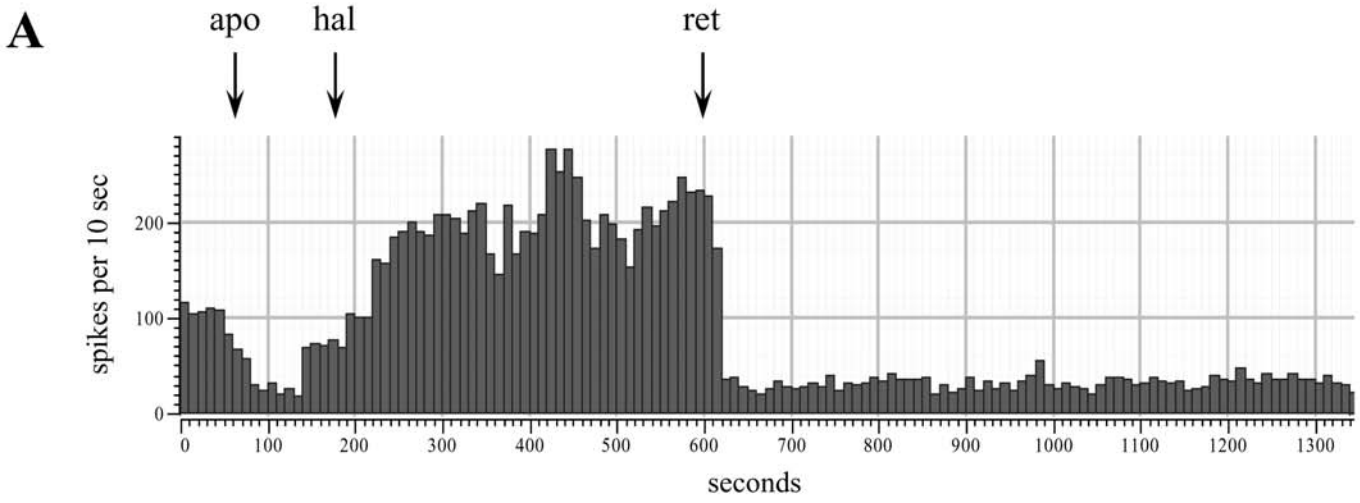

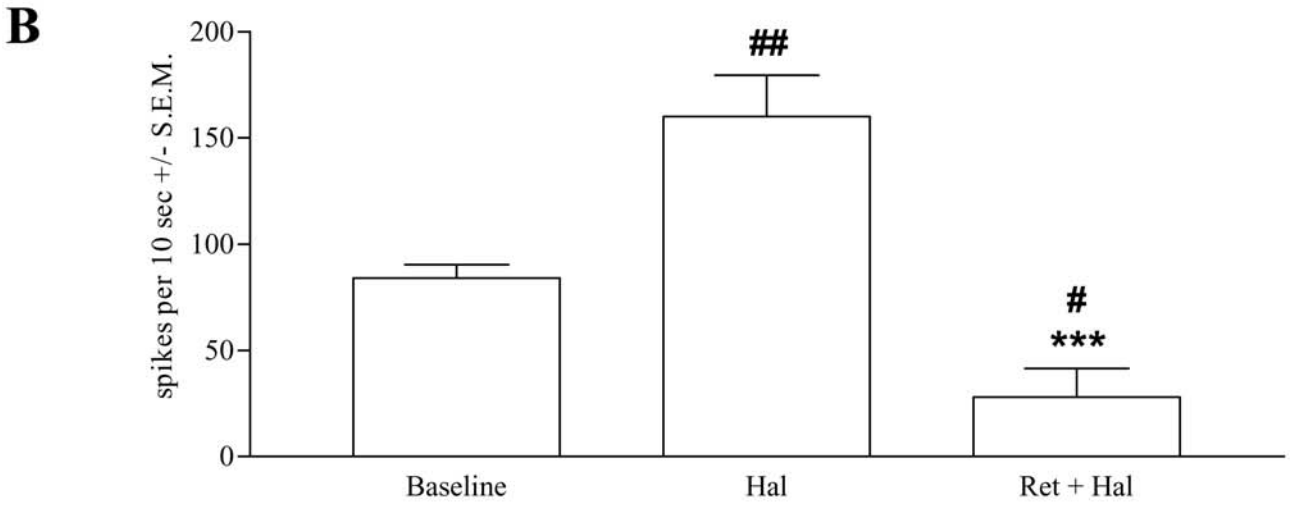

Figure 5

Figure 6

JPET Fast Forward. Published on June 14, 2006 as DOI: 10.1124/jpet.106.106757
This article has not been copyedited and formatted. The final version may differ from this version.

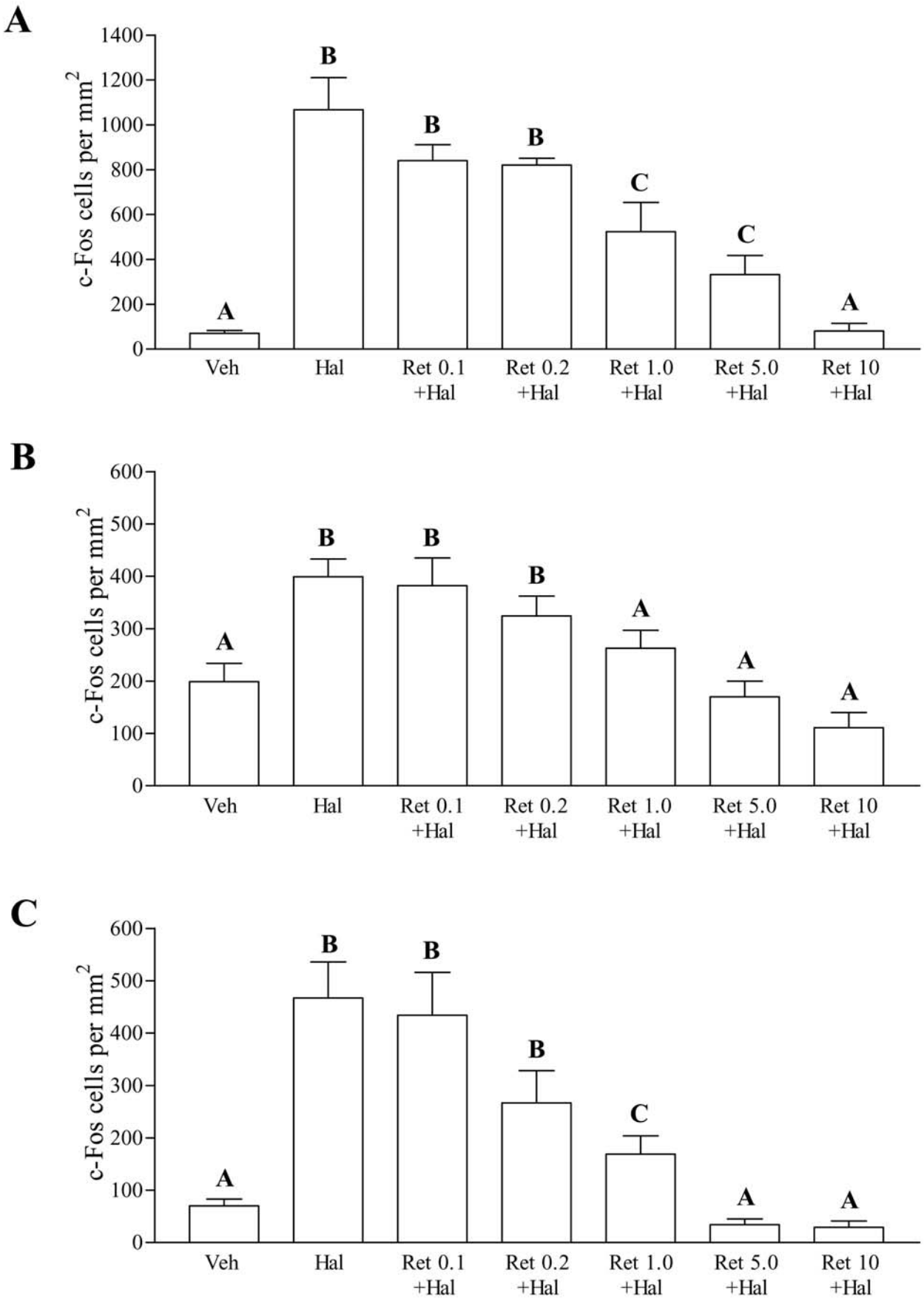

Figure 7

JPET Fast Forward. Published on June 14, 2006 as DOI: 10.1124/jpet.106.106757
This article has not been copyedited and formatted. The final version may differ from this version.

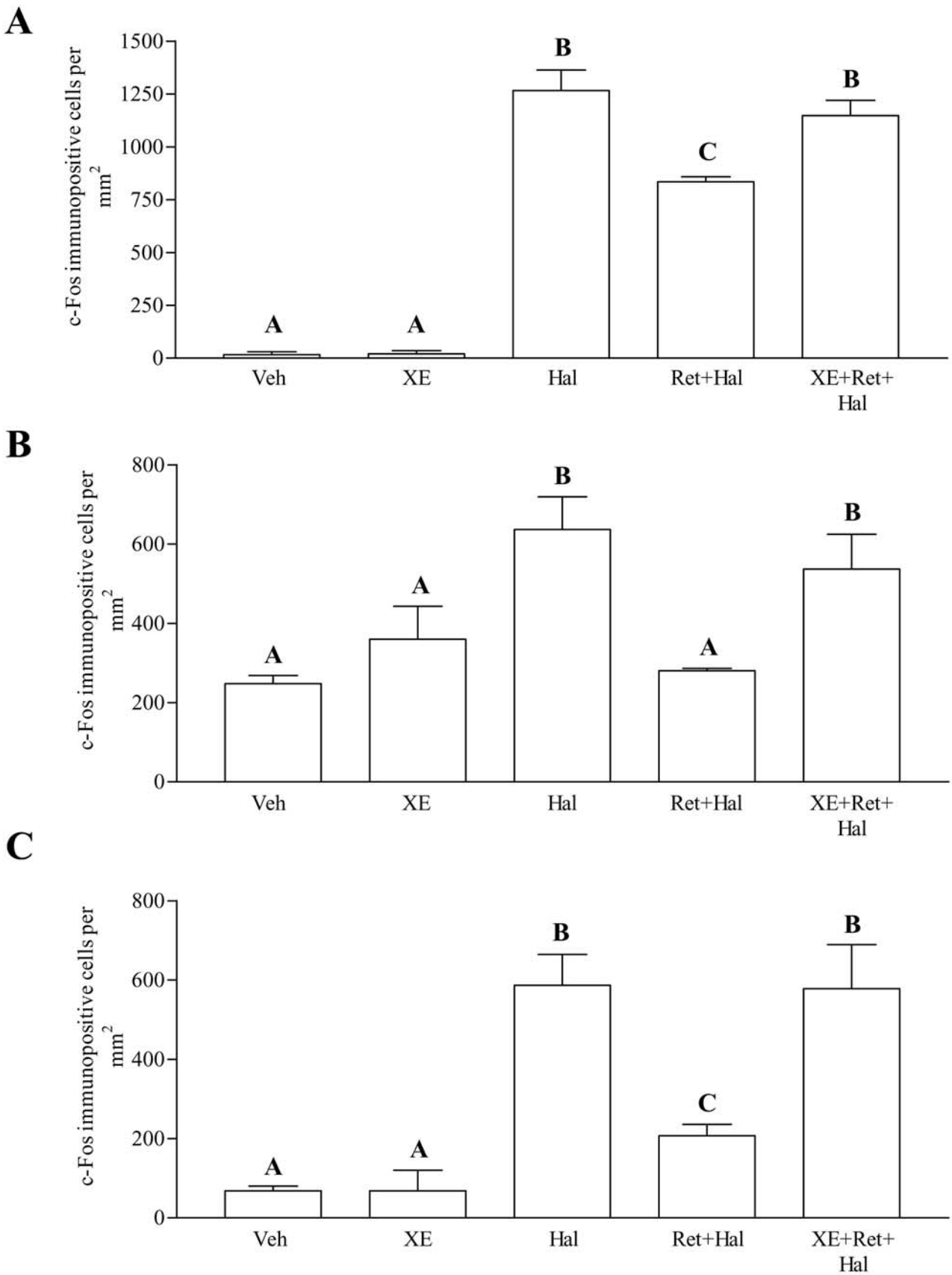

Figure 8

JPET Fast Forward. Published on June 14, 2006 as DOI: 10.1124/jpet.106.106757
This article has not been copyedited and formatted. The final version may differ from this version.

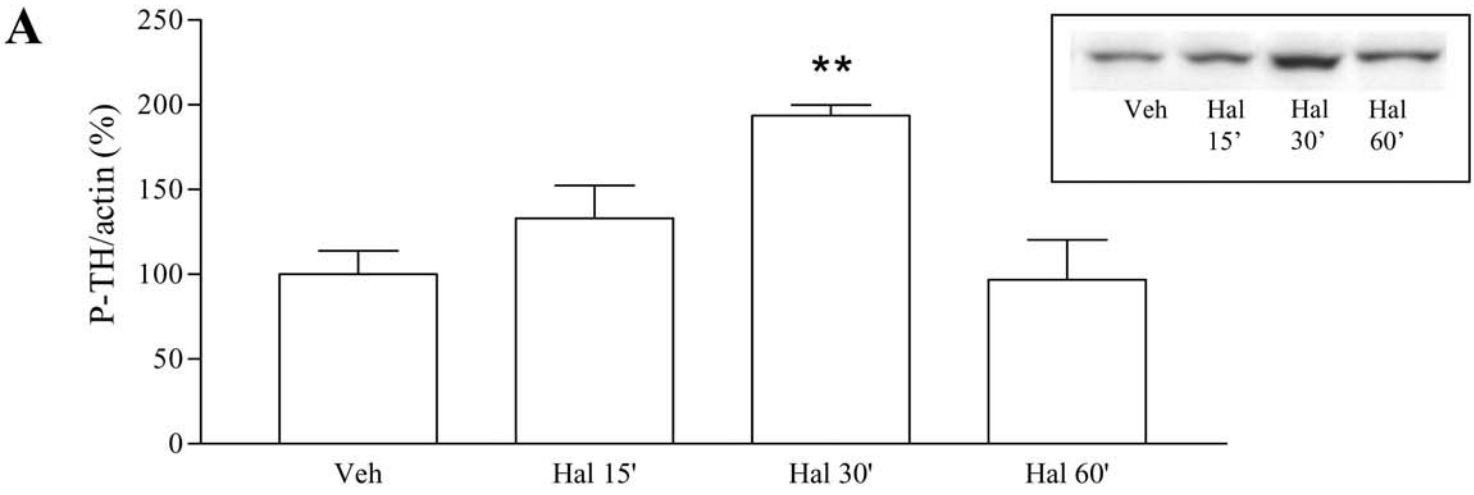

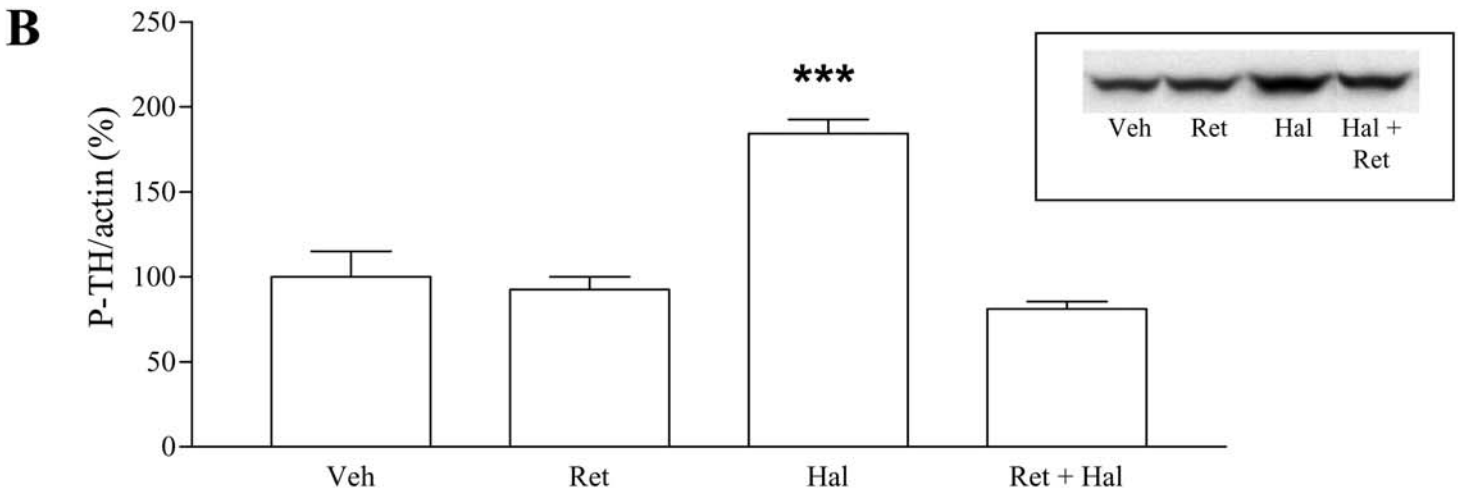

Figure 9

JPET Fast Forward. Published on June 14, 2006 as DOI: 10.1124/jpet.106.106757
This article has not been copyedited and formatted. The final version may differ from this version.

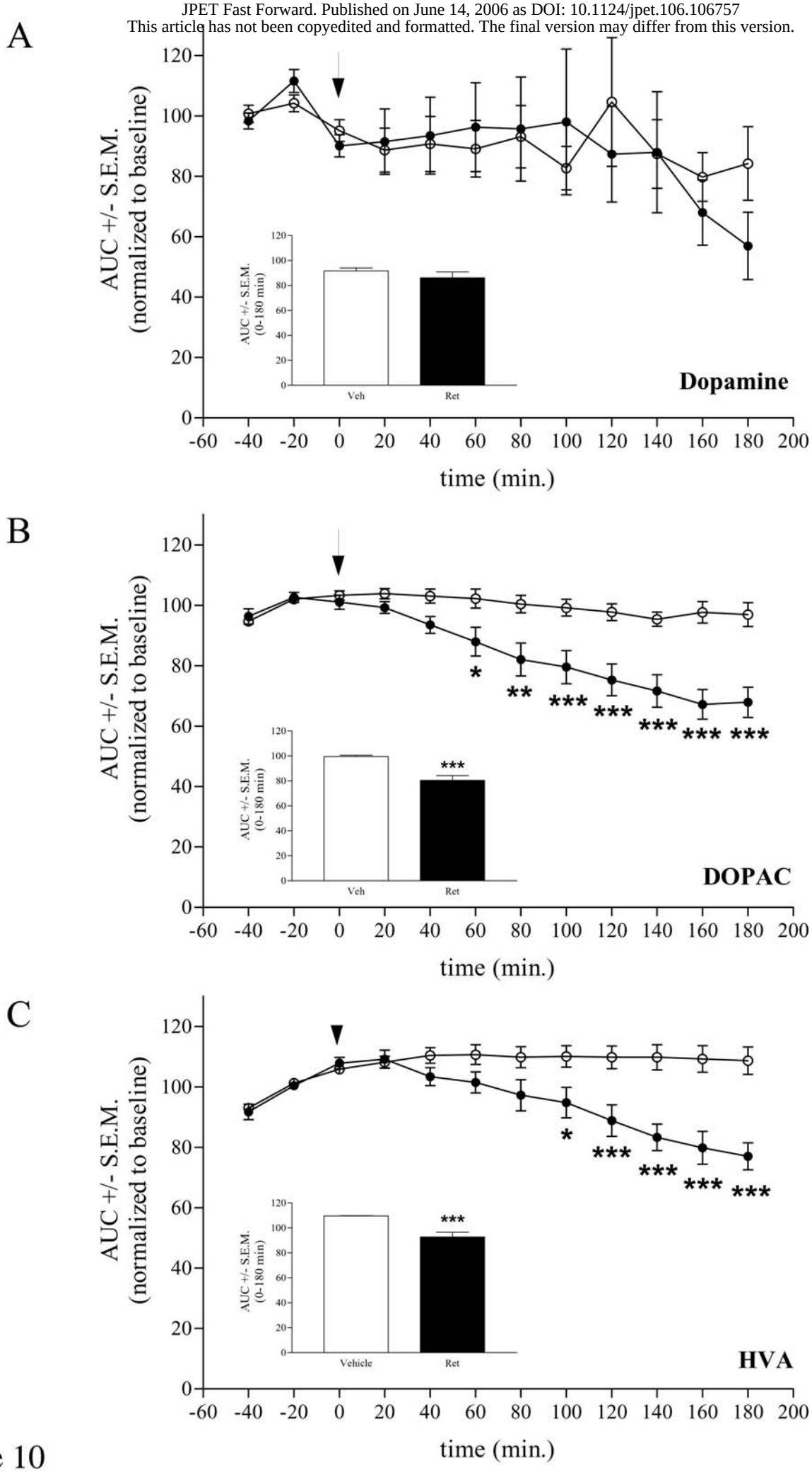

Figure 10